JOURNAL OF MATERIALS SCIENCE 27 (1992) 2101–2109

Extrusion and mechanical properties of mixed powder and spray co-deposited Al 2014/SiC metal matrix composites

M. H. CARVALHO, T. MARCELO, H. CARVALHINHOS
Laboratório Nacional de Engenharia e Tecnologia Industrial, 1699 Lisboa Codex, Portugal
C. M. SELLARS
School of Materials, University of Sheffield, Mappin Street, Sheffield S1 3JD, UK

Al 2014/SiCp metal matrix composites have been produced by a powder metallurgy route that included mixing, canning, degassing and hot extrusion (300 °C, 16:1). Two types of SiC (12 and 4 μm), two SiC contents (~ 10 vol. % and ~ 15 vol. %) and three different degassing temperatures (350, 400, 500 °C) were used. The degassing temperature was found to have no significant effect on the final properties, which were affected by remnant porosity. Porosity was mostly attributed to SiC clustering, which was related to the relative reinforcement/aluminium powder size distributions and volume fractions. The best mechanical properties were obtained for the composite with ~ 10 vol. % SiCp and these were very similar to the properties of a spray co-deposited metal matrix composite billet of approximately the same composition, also extruded at 300 °C, 16:1.

1. Introduction

The introduction of ceramic reinforcement into light metal matrices such as aluminium alloys, in order to improve specific properties, has been a subject of interest for some years because of the potential applications of these materials in the aerospace and automotive industries [1–5]. Aluminium matrix composites can be fabricated by several processing routes, the powder metallurgy (PM) route allowing more flexibility in terms of matrix, size and volume fraction of reinforcement. The PM route used in the fabrication of some of the commercially available Al/SiC composites [6, 7] always includes an outgassing/degassing step. In the PM processing of aluminium alloys, this step is well known to be critical for the achievement of good final properties [8, 9], and effective methods for evaluation of degassing have been suggested [10]. The quite different properties obtained for degassed [11] and for non-degassed [12] 2014/SiCp composites indicate that PM processing of aluminium alloys/ceramic particle composites is also affected by degassing treatments. However, information on the degassing kinetics of these types of mixtures does not seem to be available and the comparison [11, 12] could also be affected by some other differences in the processing routes used.

The present work on Al 2014/SiC particulate composites produced by PM extrusion deals with evaluation of the effect of different degassing temperatures and of the type and content of SiCp on final properties. For one given type and content of silicon carbide, comparison is made with a similar composite extruded from an ingot obtained by spray co-deposition [13], where no degassing step is involved.

2. Experimental procedure

The Al 2014 powder used in this work was provided* from overspray collected in a deposition unit that had been used for composite co-deposition. It was found to include a small amount of SiC(A), and the previous analysis for the powder [14] has been corrected accordingly to give the matrix composition shown in Table I. Two types of SiC particles F600 SIKA* and F 1200**, labelled A and B have been used for blending the powder composites. The size distributions for all the powders, determined in a Cilas 715 instrument, are shown in Fig. 1. These lead to median sizes of 78, 12 and 4 μm for the 2014, SiC(A) and SiC(B) powders, respectively.

Initial studies of the kinetics of degassing of the loose powders during continuous heating have been reported elsewhere [15]. The form of the curves obtained, particularly for water vapour evolution was unusual. It was suspected that this might have arisen partly from the experimental procedure and the particular mass spectrometer arrangement employed. The observations were therefore repeated using a different mass spectrometer and furnace arrangement [16]. Samples of powder, 0.4 g weight, were held in an aluminium boat in the furnace, which was pumped down to about 10^{-1} Pa by a separate rotary pump before being connected, initially by a capillary valve,

* Alcan International, Banbary, England.
** Struers, Copenhagen, Denmark.

0022–2461

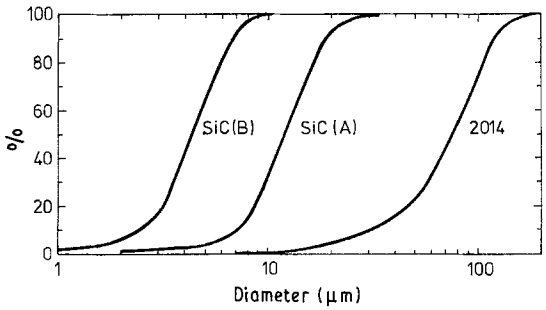

Figure 1 Cumulative size distributions of 2014 and SiC particulates.

TABLE I Analysis of 2014 alloy matrix (wt %)

	Cu	Si	Fe	Mn	Mg	Zn	O_{ppm}
Powder	4.28	0.80	0.45	0.71	0.39	0.03	294
Extrusion	4.33	0.80	0.45	0.72	0.38	0.03	347

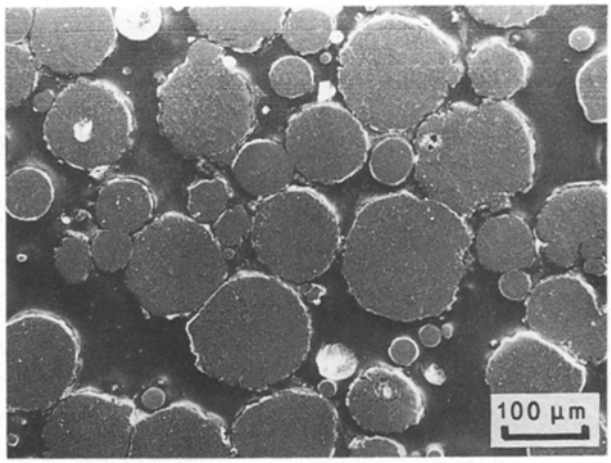

Figure 2 Scanning electron micrograph of polished 2014 powder particles.

to the main pumping system, which had been previously baked out at 500 °C. Samples were evacuated for 15 h at room temperature at 10^{-4} Pa before being heated at 2 °C min^{-1} to observe the gas evolution. All measurements of ion intensity on the powders were corrected for background obtained from heating the system by carrying an identical procedure with an empty aluminium boat.

Composite mixtures of nominally 9.3 vol. % SiC(A), 15 vol. % SiC(A) and 15 vol. % SiC(B) were prepared by dry blending for about 3 h in a Turbula tumbler. These mixtures, as well as the Al 2014 overspray powder, were processed through a conventional PM route that included canning, degassing and hot extrusion. Cans were of a similar design to those described previously [17], and made of 6082 aluminium alloy with an interior lead angle of 90° and wall thickness of 10 mm. Tapped densities in the cans were around 68% theoretical. Degassing was carried out at 350, 400 and 500 °C for 4 h, at around 10^{-2} Pa, after which the cans were sealed and air cooled.

Extrusion of the canned powder mixtures and of an uncanned spray co-deposited 9.3 vol % SiC(A) composite billet supplied by Alcan was carried out in a vertical press of 10 MN capacity. The press container was preheated to approximately 300 °C and graphite/molybdenum disulphide lubrication was used both in the container bore and on the die. Canned powder and spray co-deposited billet composites were reheated for 2 h in an air circulating furnace at 300 °C and extruded to a round bar. An extrusion ratio of 16:1 and a ram speed of around 5 mm s^{-1} were used. Some additional 10:1 extrusions were tried. Extruded bars were allowed to cool naturally in air.

Optical and scanning electron microscopy (SEM) examination was performed on polished samples of both as-extruded and as T6 heat-treated rods. The T6 treatment used was the standard one for the 2014 wrought alloy (502 °C solution treatment, water quench, 160 °C ageing for 18 h). Densities were determined by a picnometer method on 10 mm × 10 mm diameter cylinders of as-extruded and as T6 treated material. Tensile tests were carried out on T6 treated specimens of 6.4 mm diameter and 32.0 mm gauge length, in a universal testing machine, at a constant crosshead speed of 3×10^{-3} mm s^{-1}. Tensile specimens of a different geometry but also 6.4 mm diameter were machined from some of the as-extruded composites, for Young's modulus, E, determinations. E was first determined in each of those specimens in the as-extruded condition and then again after a hot isostatic pressing (315 °C, 70 Mpa, 30 min or 315 °C, 100 MPa, 2 h) and/or a T6 heat treatment as described in [18]. These tests were performed on a MTS machine, using a 25 mm gauge extensometer and strain rates of $3–4 \times 10^{-5}$ s^{-1}. Compact notched specimens from some as-extruded and as heat-treated composites were machined for mass spectrometry study of fractures, described in detail in [15]. Fracture surfaces of all the specimens tested were examined by SEM.

3. Results and discussion

The 2014 powder showed the typical near-spherical particles expected from inert gas atomisation, Fig. 2. As can be seen in this figure, some particles contained internal pores. Also, because the powder was obtained as overspray from the spray deposition unit, there was significant contamination with SiC particles. From quantitative metallographic observations on an extrusion of the alloy powder, this contamination was estimated to give a composite containing 2.4 vol % SiC. At the time when the SiC and alloy powders were weighed out to produce composites of nominal compositions 9.3 and 15.0 vol % SiC, the extent of the contamination of the alloy powder was not recognized. The actual weights employed lead to true compositions of the mixed powder composites of 10.6 and 17.1 vol % SiC.

3.1. Degassing

The results of the degassing studies on loose powders are shown in Fig. 3. The only gases detected were

water vapour, nitrogen and carbon monoxide (which have identical mass numbers and so cannot be distinguished), hydrogen and carbon dioxide. The results for the alloy powder, Fig. 3a, show a peak in water vapour evolution at 150 °C and other characteristics similar to those previously observed on other aluminium alloy powders and discussed in some detail in relation to the reactions involved [19, 20]. In the present powder, the secondary peak at about 400 °C arises mainly from nitrogen with a smaller contribution from hydrogen than has been reported previously [15]. The silicon carbide, Fig. 3b, gives general slow evolution of water vapour and nitrogen with rounded maxima at about 300 and 450 °C, respectively.

The composite powder, which was mixed in air, shows a dramatic increase in the total evolution of water vapour as seen from Fig. 3c, in which the scale for water vapour is changed by a factor of 5. The general characteristics are clearly dominated by the behaviour of the alloy powder, with small peaks in nitrogen, hydrogen and carbon dioxide being associated with the peak in water vapour evolution at 150 °C. A peak at this temperature has been reported to arise from decomposition of aluminium trihydroxide [19, 21], implying that the formation of this trihydroxide has been greatly accelerated by the tumble mixing of the powders in air.

Comparison of Fig. 3a and c shows that by 350 °C the gas evolution rate of the composite and alloy powders is similar for the species other than water vapour, which is still about twice as high in the composite. Even this difference is eliminated by 400 °C. Degassing before extrusion was carried out for 4 h at constant temperature after heating at about 2 °C min^{-1}. Measurements of pressure in the primary vacuum system during heating of the canned composite powder show a characteristic variation illustrated in Fig. 4. The peaks at $\simeq$ 150 and 350 °C correspond closely with the peaks in ion intensity in Fig. 3. Previous mass spectrometer observations on small samples of loose powders [17] indicated that isothermal degassing for about 1 h at the temperatures employed should reduce the evolution rates to very low levels. Pressure measurement in the vacuum system confirm this, e.g. for degassing at 400 °C pressure fell from $\simeq$ 5 Pa to $\simeq 10^{-2}$ Pa within 1 h of the temperature being reached, and then only decreased to $\approx 5 \times 10^{-3}$ Pa in the remaining 3 h.

3.2. Extrusion

The alloy powder and mixed powder composites all showed the same characteristic shape of extrusion pressure–distance curves described previously for extrusion of 7075 powders [17]. Somewhat surprisingly, no systematic differences in the pressures were found for the different volume fractions, or type of SiC, or for the different degassing treatments. The curve given in Fig. 5 for the 10.6% SiC mixed powder composite is thus typical in form for all the powder extrusions. The initial upset distance (l) does vary somewhat because of variations in tap density with composition, being 62% for the alloy powder, 65% for 10.6 vol. % SiC (A), 68.5% for 17.1 vol. % SiC (A) and 74% for 17.1 vol. % SiC (B). It is noteworthy that all these tap densities are high compared with general experience, probably because of the long tail to small particle sizes in the alloy powder, Fig. 1, and the efficient packing of the bimodal sizes of the mixed powders, particularly SiC(B). From a practical viewpoint, these high packing densities are beneficial in giving a good yield of extrusion and in minimizing instabilities in can wall thickness that can develop during upsetting.

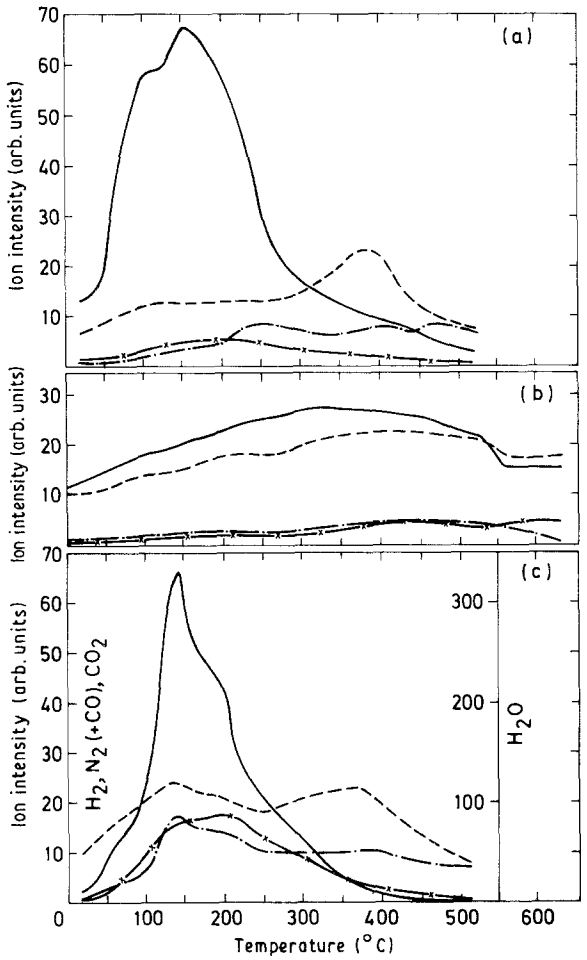

Figure 3 Degassing kinetics on heating at 2 °C min^{-1}: (a) 2014, (b) SiC (A), (c) 2014 + 17.1 vol.% SiC (A) powders, determined after 15 h degassing at room temperature to attain an initial vacuum of 10^{-4} Pa. (——) H_2O, (—— · ——) H_2, (– – –) N_2 (+ CO), (— × —) CO_2.

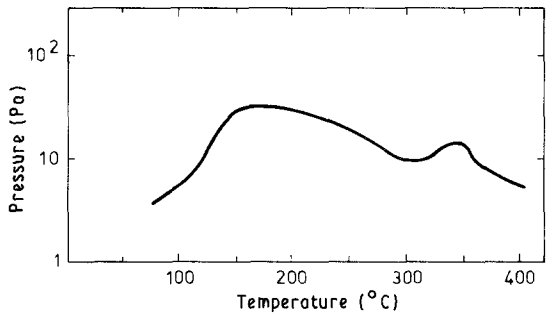

Figure 4 Pressure variation in the primary vacuum circuit during heating of a canned composite powder for degassing at 400 °C.

The pressure (2) in Fig. 5 corresponds to breakthrough of the front end of the can, (3) to the start of steady state extrusion of the composite and (4) to the start of the back-end defect created by the can end being drawn into the centre of the composite [17]. The lack of systematic effect of different SiC contents on the pressure between (3) and (4) is not understood, but may indicate that shear occurs easily at the matrix/SiC interfaces, so negating the expected strengthening from the SiC particulate. The curve in Fig. 5 corresponding to the uncanned spray co-deposited billet shows the typical steep rise in pressure during upset of solid billets, followed by a high breakthrough pressure and then a fall to essentially the same steady state value as for the mixed powder composites. In all cases, including the uncanned spray co-deposited billet, the extruded bar had a satisfactory surface finish and no deterioration of the die was observed.

3.3. Microstructure and porosity

All the extrusions showed reasonably homogeneous distributions of SiC particles in transverse sections, but, as shown in Fig. 6, some banding and clustering was apparent in longitudinal sections, particularly with 17.1 vol. % SiC(B), Fig. 6e. Scanning microscopy of the extrusions of mixed powders, e.g. Fig. 7, and of the co-deposited billet, Fig. 8 showed the development of voids at the interfaces of isolated SiC particles. These were most common at interfaces transverse to the extrusion direction. Clustering of SiC particles also resulted in incomplete local consolidation during extrusion, Figs 7b and 8b. The other feature apparent in these figures is the presence of coarse particles of $CuAl_2$ phase initially formed on cooling after atomization/spray deposition and undissolved on subsequent heating for degassing/extrusion. In the mixed powder composites, these particles were homogeneously distributed, Fig. 7, whereas in the spray co-deposited composite, coarse particles were frequently found to have formed at the SiC particle interfaces, Fig. 8.

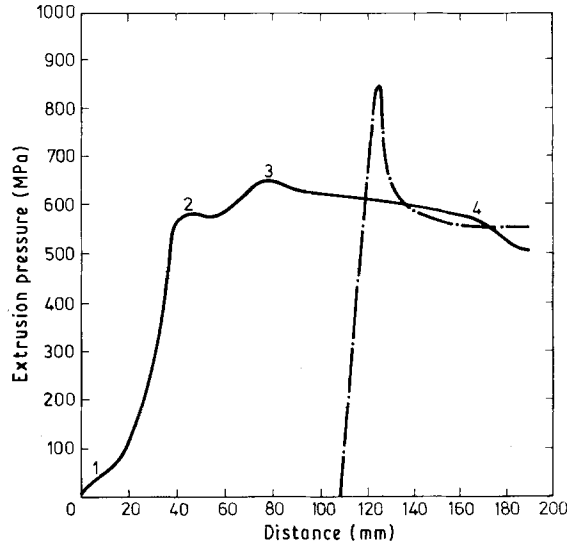

Figure 5 Typical extrusion pressure–distance curves for (—) mixed powder and (——·——) spray co-deposited composites.

Densities measured on the as-extruded bars and on the same samples after heat treatment to the T6 condition are shown in columns 2 and 3 of Table II. In general it can be seen that the heat treatment leads to a small decrease in density. Scanning electron microscopy, e.g. Fig. 9, revealed that the decrease in density arises from the development of small pores in the matrix, not associated with SiC particles. These are less frequent in the spray co-deposited composite, Fig. 9a, than in the mixed powder composites, Fig. 9b. Furthermore, on fracturing solution-treated samples in the mass spectrometer [15], significant gas evolution was observed from the mixed powder composite, but not from the spray co-deposited composite, Fig. 10. The degassing treatment at 500 °C given to the mixed powder composite before extrusion is expected to remove nearly all the absorbed gases on the powder surfaces, so the gas evolution on fracture is attributed to gas entrapped in internal pores in some of the powder particles, Fig. 2. Fig. 10a then indicates that gas entrapment is much less serious in spray co-deposition. However, expansion of the entrapped gases on solution treatment at 502 °C is considered to be the cause of the decrease in density and the appearance of isolated voids shown in Fig. 9 in the heat-treated bars.

The theoretical density, ρ_T, of the different composites, calculated by the law of mixtures assuming a relative density of 3.21 for SiC, is shown in Table III. These values and the observed densities, ρ_o, given in Table II have been used to determine the volume per cent of pores, p, as

$$p = 100(1 - \rho_o/\rho_T) \quad (1)$$

The results, given in Table III, show that minimum porosity is present in the spray co-deposited composite and the maximum occurs in the 17.1 vol. % SiC(B) composite in the heat-treated condition. These results are entirely consistent with the qualitative descriptions given earlier from the micrographs and show that porosity associated with clusters of SiC particles makes a major contribution to overall porosity.

3.4. Elastic modulus

The values of Young's modulus determined on the extruded composites in the T6 condition are shown in Table II. Other results for the extruded condition, showing the effects of subsequent hot isostatic pressing and T6 heat treatment are reported elsewhere [18]. It was noted that hot isostatic pressing caused metal flow into the voids associated with clusters of SiC particles and increased the density of the composites. From the highest values of modulus obtained in this work, the effective Young's modulus for the SiC particulate was estimated from a law of mixtures to be $\simeq$ 250 GPa. This is considerably lower than the value of 482 GPa or 551–1033 GPa reported for SiC whiskers [22], but is consistent with values of 180–220 GPa observed for yarn/fibre [23]. Furthermore an equivalent difference has been observed between the modulus of alumina whiskers and Saffil

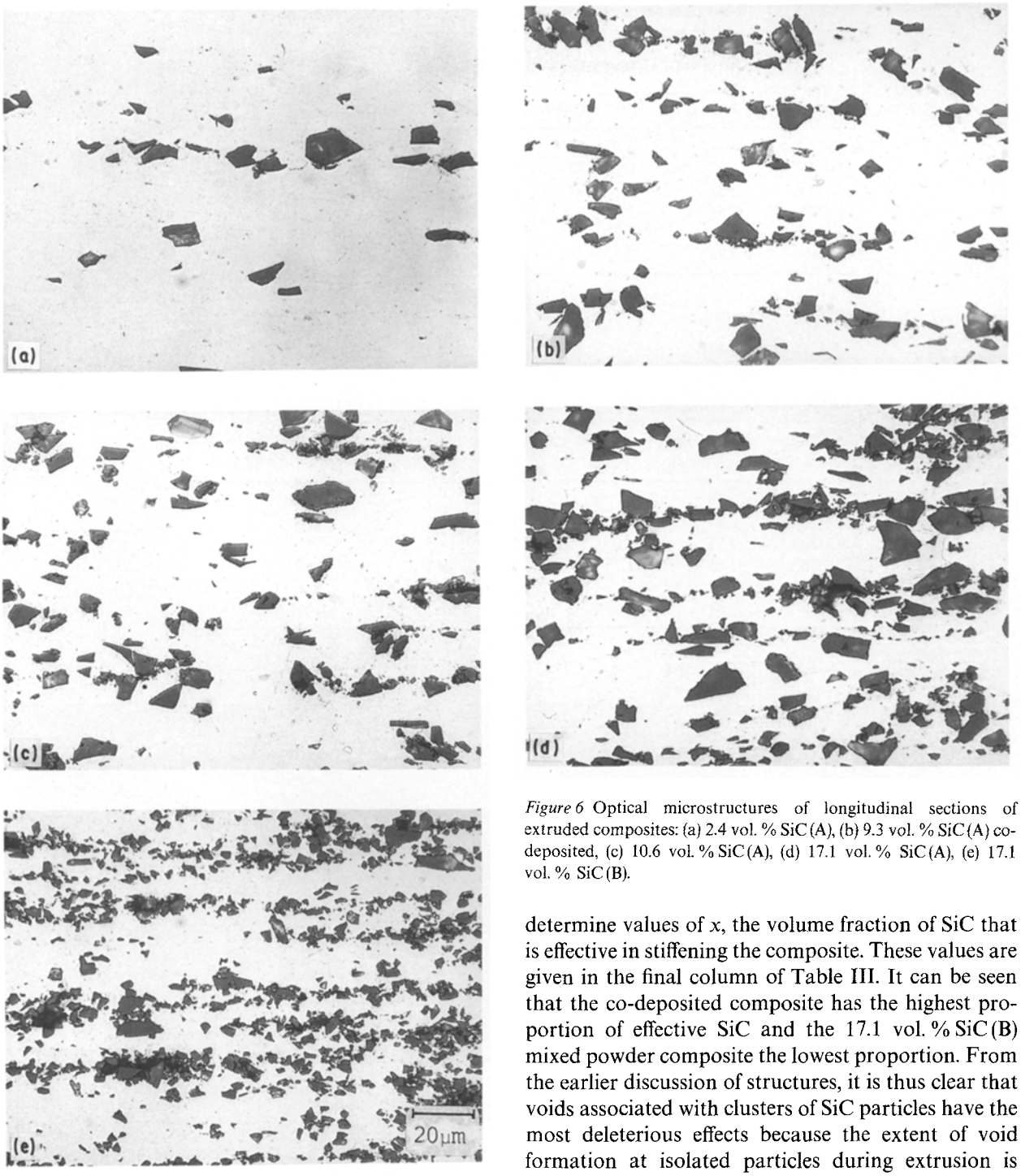

Figure 6 Optical microstructures of longitudinal sections of extruded composites: (a) 2.4 vol. % SiC(A), (b) 9.3 vol. % SiC(A) co-deposited, (c) 10.6 vol. % SiC(A), (d) 17.1 vol. % SiC(A), (e) 17.1 vol. % SiC(B).

fibres [22, 23]. Theoretical values of Young's modulus have been calculated for the composites by the law of mixtures as

$$E_{comp} = 72.4(1 - x - p) + 250(x) + 0(p) \quad (2)$$

where x and p are the volume fractions of SiC and pores, respectively. These theoretical values are shown in Table III and are consistently higher than the measured values in Table II. As discussed earlier, the majority of voids in both the extruded and heat-treated conditions are associated with transverse interfaces of SiC particles or with clusters of particles. If it is considered that such SiC particles are rendered ineffective and act like voids during the determination of Young's modulus, the experimental values of modulus for the composites can be used in Equation 2 to determine values of x, the volume fraction of SiC that is effective in stiffening the composite. These values are given in the final column of Table III. It can be seen that the co-deposited composite has the highest proportion of effective SiC and the 17.1 vol. % SiC(B) mixed powder composite the lowest proportion. From the earlier discussion of structures, it is thus clear that voids associated with clusters of SiC particles have the most deleterious effects because the extent of void formation at isolated particles during extrusion is similar in all cases.

3.5. Tensile properties

The tensile properties of all the composite materials were determined after T6 heat treatment. The results for the 350, 400 and 500 °C degassing temperatures were found to be closely reproducible, so only mean values for the different compositions are reported in Table II. Comparison of the properties with those expected for 2014, also shown in Table II indicate some enhancement in strength at the expense of ductility up to 10.6 vol. % SiC, with the mixed powder and spray co-deposited composites giving closely similar results. With higher volume fractions, there is a deterioration in properties, which is attributed to the increased clustering of the SiC particulate, particularly evident in the 17.1 vol. % SiC(B) composite.

TABLE II Density and mechanical properties of experimental composites

Material (vol % SiC)	Relative density		Young's modulus	Proof strength	Tensile strength	Elong.
	As-ext	T6	(MPa)	(MPa)	(MPa)	(%)
0[a]	–	2.80	72.4	414	483	13.0
2.4(A)	2.77	2.76	73	429	490	11.6
9.3(A)[b]	2.82	2.82	84	468	516	4.1
10.6(A)	2.81	2.79	79	466	517	4.1
17.1(A)	2.78	2.77	85	457	488	1.3
17.1(B)	2.74	2.71	73	411	439	0.8

[a] [24].
[b] Spray co-deposited.

TABLE III Porosity and volume percentage of effective SiC in extruded composites

Material (vol. % SiC)	Theoretical rel. density	Porosity (%) As. Ext	T6	Theoretical modulus (GPa)	"Effective" (vol. % SiC)
0	2.80	–	–	72.4	–
2.4(A)	2.80	1.1	1.4	75.6	1.3
9.3(A)[a]	2.84	0.6	0.6	88.5	7.5
10.6(A)	2.85	1.3	2.0	89.8	6.3
17.1(A)	2.87	3.1	3.5	100.2	11.0
17.1(B)	2.87	4.5	5.6	98.7	6.8

[a] Spray co-deposited.

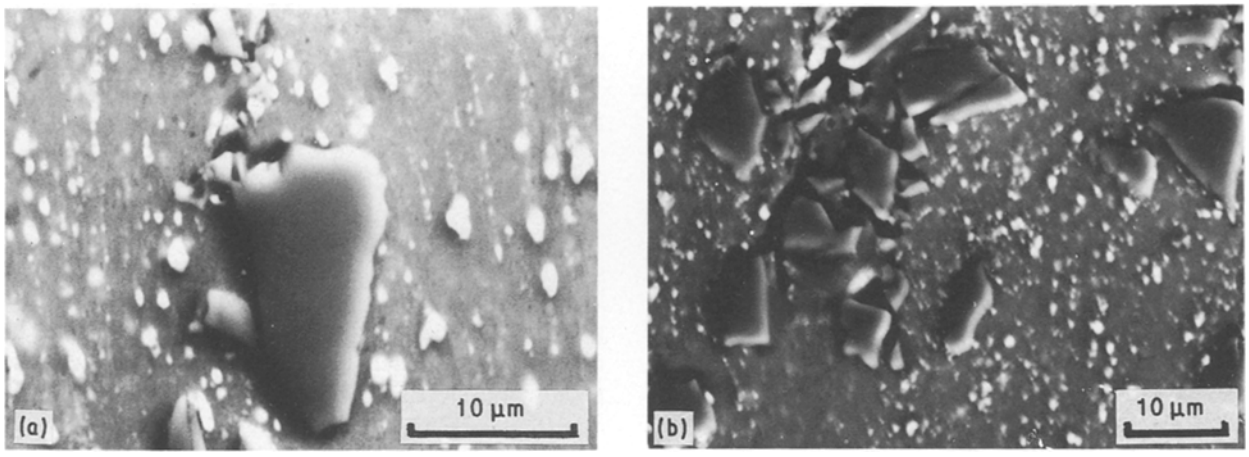

Figure 7 Scanning electron micrographs of longitudinal sections of extruded powder composites: (a) 17.1 vol. % SiC (A), degassed at 400 °C, (b) 10.6 vol. % SiC (A), degassed at 350 °C, showing voids at the ends of individual SiC particles and within clusters.

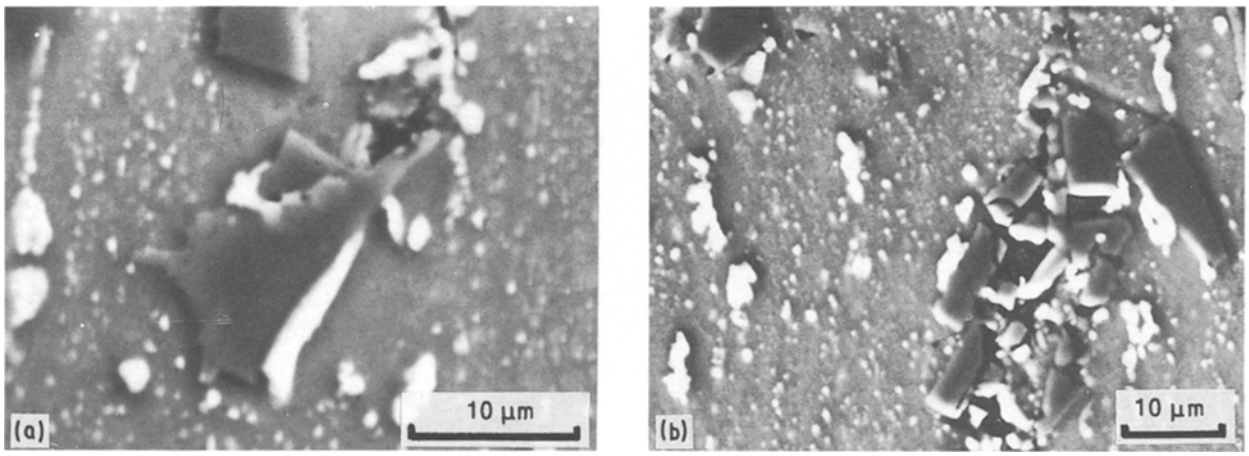

Figure 8 Scanning electron micrographs of longitudinal sections of extruded spray co-deposited 9.3% SiC vol. (A), showing void formation similar to Fig. 7 and frequent precipitation of the $CuAl_2$ phase at the SiC particles.

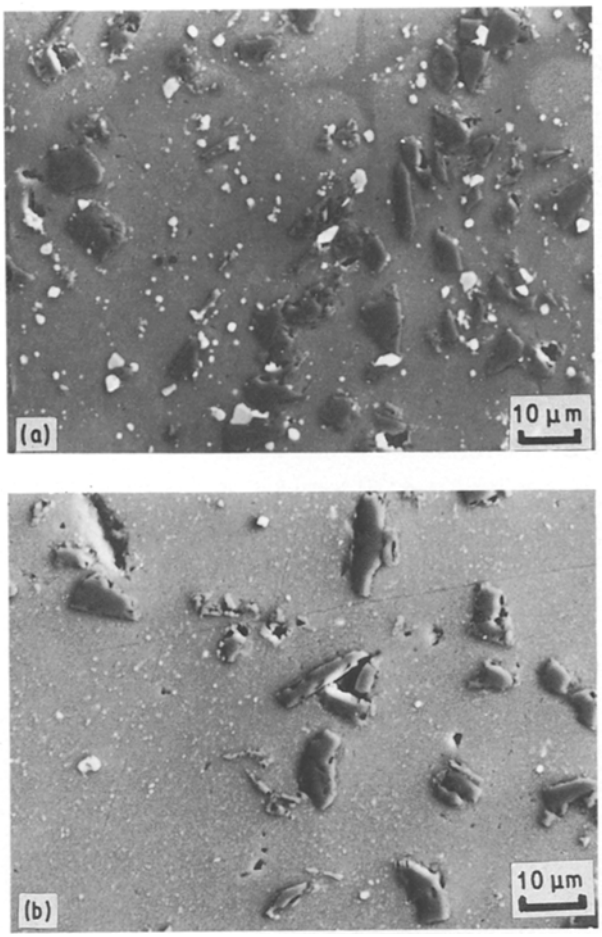

Figure 9 Scanning electron micrographs of extrusions heat treated to the T6 condition: (a) spray co-deposited 9.3 vol. % SiC(A) and (b) mixed powder 10.6 vol. % SiC(A), degassed at 400 °C.

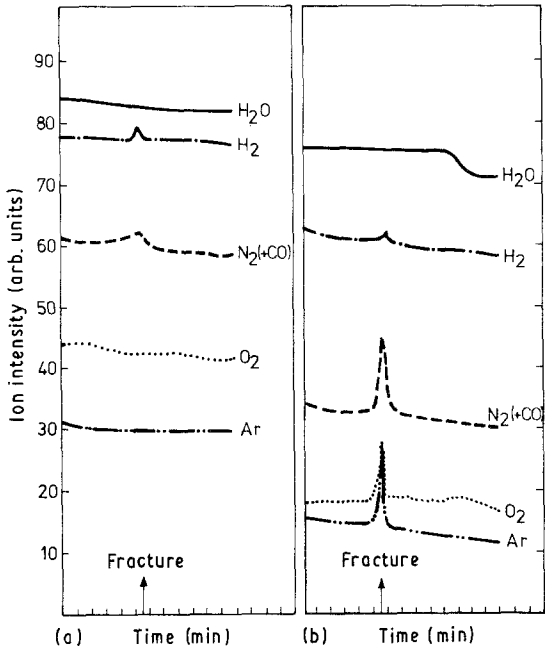

Figure 10 Gases detected on rupture of extrusions tested in the solution heat-treated condition (502 °C, 35 min): (a) spray co-deposited 9.3 vol. % SiC(A) and (b) mixed powder 17.1 vol. % SiC(A) degassed at 500 °C prior to extrusion. Total pressure in mass spectrometer chamber 10^{-3} Pa.

Scanning electron microscopy of the tensile fracture surfaces show similar characteristics for all composites, with the majority of SiC particles either intact or not present, indicating that debonding has occurred at the particle/matrix interfaces. However, some SiC particles were fractured and showed occasionally adherent matrix, indicative of good local interface bonding. Examples are shown in Fig. 11, from which it can be seen that between the SiC particles the matrix exhibits dimpled intragranular fracture, with no evidence of intergranular separation between the original powder particles. Extrusion at 300 °C and 16:1 extrusion ratio thus appears to be satisfactory for bonding the alloy matrix particles. Other extrusions, not reported in detail here, which were carried out with an extrusion ratio of 10:1 showed extensive debonding between matrix powder particles on tensile testing, indicating that 16:1 is probably near the minimum satisfactory extrusion ratio for this material. The matrix fractures in Fig. 11 show more, smaller dimples in the mixed powder composite, Fig. 11a. This is a direct consequence of the difference in distribution and size of the intermetallic particles that remain out of solution during solution treatment, as seen in Fig. 9.

The results indicate an optimum content of about 10 vol % SiC for the process routes adopted for this work because increased clustering of SiC particles and the associated voids negate any benefits from larger

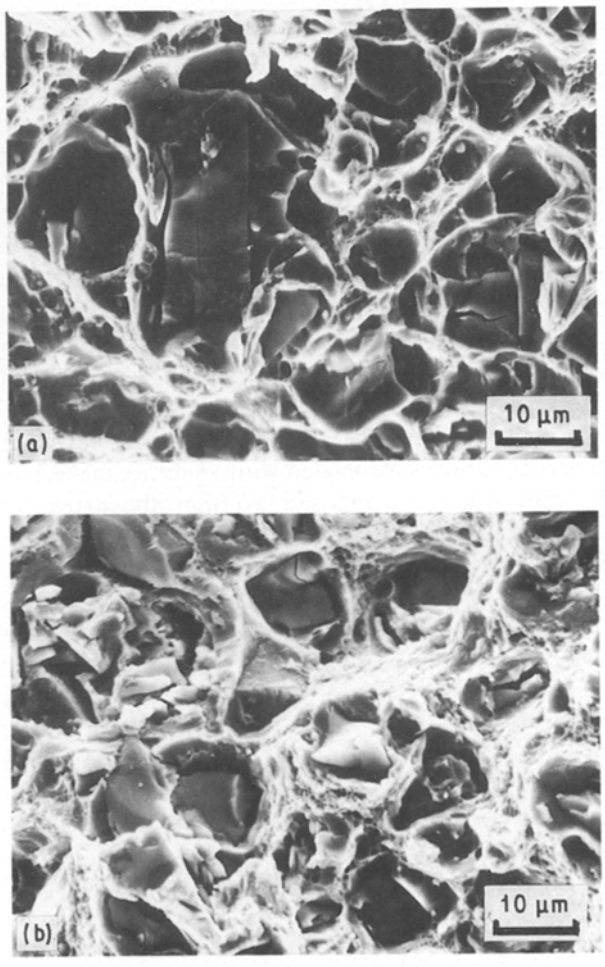

Figure 11 Scanning electron micrographs of tensile fracture surfaces of extruded and T6 heat treated composites, (a) spray co-deposited 9.3 vol. % SiC(A) and (b) mixed powder 10.6 vol. % SiC(A) degassed at 350 °C.

additions. Overall, the mechanical properties achieved in the composites are disappointing and appear to be limited by the presence of porosity. Even in the absence of clusters of SiC particles, extrusion at 300 °C creates voids at isolated particles so that 100% density cannot be achieved. The extrusion of similarly processed 2014/SiCp composites carried out at 450 °C by Jokinen [11] apparently yielded denser products with higher elongation and Young's modulus but lower tensile and yield strengths than those reported in the present work.

However, it is noteworthy that with this limitation, composites produced by the spray co-deposition route give identical results to those from the mixed powder route which involves many more steps.

4. Conclusions

1. During heating of the 2014 powder in vacuum there was a major peak in evolution of water vapour at $\simeq 150$ °C, which is typical of aluminium alloy powders, but a secondary peak at $\simeq 400$ °C arises mainly from nitrogen rather than hydrogen in the present work.

2. The degassing characteristics of the mixed alloy + SiC powders were essentially similar to those for the alloy powder, but with a significantly higher release of water vapour.

3. The extrusion pressure ram travel curves at 300 °C, 16:1, for all the mixed powder composites were essentially identical, with no systematic effect on pressure of the different contents or type of SiC and no effect of the different prior degassing treatments at 350, 400 and 500 °C.

4. All the extrusions showed some voids at SiC interfaces, particularly those transverse to the extrusion direction, with additional voiding associated with clusters of SiC particles. The clustering increased with volume fraction of SiC and was worst with 17.1 vol % fine SiC particulate, leading to a total porosity of about 4.5% in the extrusions.

5. Measurements of Young's modulus indicated that SiC particles associated with voids are ineffective in stiffening the composite, so that the extent of clustering of SiC is of critical importance in determining their effective volume fraction.

6. For the present powders and process routes $\simeq 10$ vol % SiC appears to be the optimum, with the composite produced by spray co-deposition showing somewhat less clustering than those produced from mixed powders.

7. With about 10 vol % SiC, the two process routes of spray co-deposition or powder mixing followed by extrusion and heat treatment lead to nearly identical mechanical properties.

The present work indicates that elimination of SiC particle clustering and attainment of 100% density by either process route is essential if the potential properties of the composite materials are to be reached in practice. Process conditions that will give 100% density are also needed to evaluate fully the effect of degassing in PM composites.

Acknowledgements

Travel expenses were supported by AGARD/NATO. Peter Clarke and David Braine, Sheffield University, M. Durand, Ecole des Mines de Paris, Lia Soares, Luis Fernandes, Augusto Geraldes and Mário Melo, LNETI, are thanked for help with the experimental work. Drs J. P. Henon and Michel Jeandin, Ecole des Mines de Paris, M. P. Silva, Sheffield University, J. Moutinho, Universidade Nova de Lisboa, are also thanked for their contributions to MSA experiments and their interpretation.

References

1. S. V. NAIR, J. K. TIEN and R. C. BATES, *Int. Met. Rev.* **30** (1985) 275.
2. J. P. ROCHER, F. GIROT, J. M. QUENISSET, R. PAILLER and R. NASLAIN, *Mem. Etudes Sci./Rev. Métall.* **2,** February (1986) 69.
3. J. A. CORNIE, Y-M. CHIANG, D. R. UHLMANN, A. MORTENSEN and J. M. COLLINS, *Ceram. Bull.* **65** (1986) 293.
4. P. K. ROHATGI, R. ASTHANA and S. DAS, *Int. Met. Rev.* **31** (1986) 115.
5. S. J. HARRIS, *Mater. Sci. Technol.* **4** (1988) 231.
6. D. L. ERICH, *Int. J. Powder Metall.* **23** (1987) 45.
7. H. J. RACK and P. W. NISKANEN, *Light Metal Age* **42,** February (1984) 9.
8. L. ACKERMAN, L. GUILLEMIN, R. LALAUZE and C. PIJOLAT, in "High Strength Powder Metallurgy Aluminium Alloys II", edited by G. J. Hildeman and M. J. Koczak, (TMS AIME Warrendale, PA, 1982) pp. 175–91.
9. F. H. FROES and J. R. PICKENS, *J. Metals* **36,** January (1984) 14.
10. S. D. KIRCHOFF, J. Y. ADKINS, W. M. GRIFFITH and I. A. MARTORELL, ASTM Special Technical Publication 890 (American Society for Testing and Materials, Philadelphia, PA, 1986) pp. 354–66.
11. A. JOKINEN, "Modern Developments in Powder Metallurgy", Proceedings of the International Powder Metallurgy Conference, Orlando, Florida, June 1988, Vol. 19 (MPIF/APMI, 1988) pp. 547–63.
12. B. ROEBUCK and A. E. J. FORNO, *ibid.*, Vol. 20, pp. 451–65.
13. T. C. WILLIS, J. WHITE, R. M. JORDAN and I. R. HUGHES, in "Proceedings of the International Conference on PM Aerospace Materials", Luzern, November 1987 (MPR, Shrewsbury, 1988) 29.1–29.13.
14. M. H. CARVALHO, T. MARCELO, H. CARVALHINHOS and C. M. SELLARS, in "Proceedings of the VII International Conference on Composite Materials", Vol. 1, Guangzhou, China, November 1989, edited by W. Yunshu, G. Zhenlong and W. Renjie, (International Academic, 1989) pp. 491–6.
15. T. MARCELO, M. H. CARVALHO, H. CARVALHINHOS, J. P. HENON and M. JEANDIN, *ibid.*, pp. 497–502.
16. M. P. SILVA, H. JONES and C. M. SELLARS, in "Proceedings of the International Conference on Powder Metallurgy", Vol. II, London, July 1990 (Institute of Metals, 1990) pp. 315–18.
17. M. H. CARVALHO, H. CARVALHINHOS, and C. M. SELLARS, *Powder Metall.* **33** (1990) 339.
18. J. FAUSTINO, T. MARCELO, M. H. CARVALHO and H. CARVALHINHOS, in "Proceedings of the International Conference on Powder Metallurgy", Vol. II, London, July 1990 (Institute of Metals, London, 1990) pp. 293–7.
19. J. T. MORGAN, H. L. GEGEL, S. M. DOREIVELU and L. E. MATSON, in "Proceedings of the AIME Symposium on High Strength Powder Metallurgy Aluminium Alloys", Dallas, TX, February 1982, edited by M. J. Koczak and G. J. Hildeman (American Institute of Mining Metallurgical and Petroleum Engineers, Warrendale, PA, 1982), pp. 193–206.

20. H. SCHLICH, M. THUMAN and G. WIRTH, in "Proceedings of the International Conference on PM Aerospace Materials', Luzern, November 1987 (MPR, Shrewsbury, 1988) 13.1–13.19.
21. A. I. LIVINTSEV and L. A. ARBUZOVA, *Sov. Powder Metall. Met. Ceram.* **1** (1967) 1.
22. W. J. SMOTHERS (ed) *Ceram. Source* **I** (Am. Ceram. Soc., Columbus, OH, 1986) 296.
23. K. SCHULTE and W. BUNK, in AGARD Conference Proceedings no. 444, "New light alloys", Mierlo, Netherlands, October 1988 (AGARD, Paris 1989), 26.1–26.16.
24. H. BAKER, D. BENJAMIN and C. W. KIRKPATRICK (eds) "ASM Metals Handbook", Vol. 2, 9th Edn (American Society Metals, Metals Park, OH, 1979) p. 71.

Received 10 December 1990
and accepted 15 January 1991